



**INFN/code-98/001**  
**October 4, 2007**

**MEASUREMENT OF THE FREQUENCY RESPONSIVITY OF A FIBER OPTIC  
AIR BACKED MANDREL HYDROPHONE UP TO 10 KHZ IN AIR**

M.Anghinolfi<sup>1</sup>, A.Bersani<sup>1</sup>, A.Calvi<sup>3</sup>, A.Cotrufo<sup>3</sup>, M.Ivaldi<sup>1</sup>, O.Ershova<sup>2</sup>, F.Parodi<sup>1</sup>,  
D.Piombo<sup>1</sup>, A.Plotnikov<sup>2</sup> and L.Repetto<sup>3</sup>

<sup>1)</sup> *INFN-Sezione di Genova, Via Dodecaneso 33, I-16146 Genova, Italy*

<sup>2)</sup> *Moscow State University, 119992 Moscow, Russia*

<sup>3)</sup> *Università degli Studi di Genova, Dipartimento di Fisica,  
Via Dodecaneso 33, I-16146 Genova, Italy*

**Abstract**

We describe the measurements which we have conducted to determine the responsivity of our prototype fiber optic hydrophone in air in the frequency range up to 10 kHz. Hydrophone calibration was performed with the help of a microphone with a known frequency response characteristic. Hydrophone responsivity was found to be flat within  $\pm 6$  dB in the given frequency range. We also studied the minimum pressure amplitude detectable by our hydrophone in air.

PACS.: 43.38.Pf

*Presented at the  
Workshop of the Russian-Italian collaboration in the Cosmic Ray Physics, Moscow  
October 17 2005*

*Published by SIS-Pubblicazioni  
Laboratori Nazionali di Frascati*

## 1 OUTLINE

In the previous reports<sup>1), 2)</sup> we determined the optimal geometry of an air backed fibre optic hydrophone in order to achieve the required bandwidth and responsivity<sup>1)</sup>, we discussed the characteristics of the chosen materials and we described in detail the realization of a prototype, including the procedure of winding the optic fiber and the coating process<sup>2)</sup>.

The aim of the measurements reported here was to study a frequency response characteristic of the hydrophone, particularly in absolute units. Hydrophone calibration was performed with the help of a microphone with a known frequency response characteristic. The result was averaged over 3 spatial positions of the hydrophone inside a box with proper shielding in order to reduce the influence of an interference pattern induced by sound reflections from the walls of the measuring chamber.

In the following analysis we compared the response characteristics of the microphone and the hydrophone in our particular experimental conditions, and, knowing the absolute pressure values from the microphone calibration information, we figured out the absolute hydrophone frequency response in [dB re rad/ $\mu$ Pa] units. Knowing the absolute signal value in Pa, we have also determined the minimum pressure detectable by our hydrophone. This has been done by analyzing the noise level and assuming that a signal is detectable if its amplitude exceeds  $(\mu + 3\sigma)$  level of normally distributed noise.

## 2 EXPERIMENTAL SET-UP

During the measurements the hydrophone and the microphone were placed in a box of cubic shape with inside volume of approximately 70x70x70 cm. This chamber provided isolation from external noises. Inner walls of the chamber were designed as a pattern of regularly located foam wedges in order to absorb incident sound waves and reduce reverberation effects. During the measurements it was found out that the chamber was not actually anechoic. So the main function of the chamber was isolation from external noises.

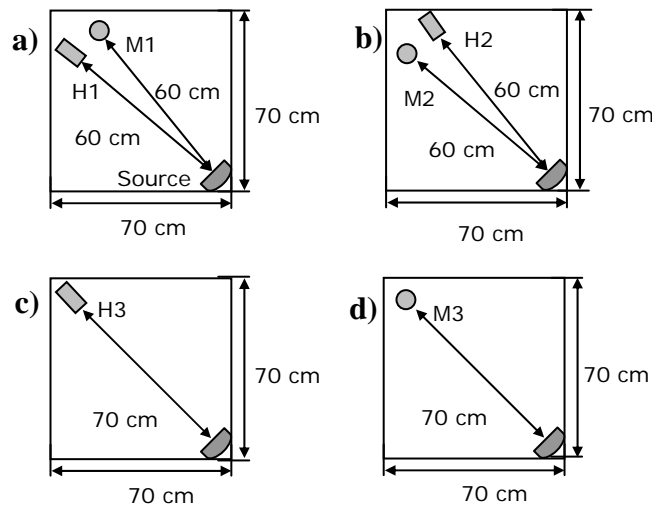


**FIG. 1:** Experimental set-up.

Measurements were performed for 4 different arrangements of sound detectors inside the chamber, which are shown in fig.1. In cases a) and b) the data was recorded from both the hydrophone and the microphone at one time. Their positions in a) and b) were swapped and were supposed to be symmetrical with respect to the diagonal of the chamber (within a set-up accuracy available in our experiment). The influence of interference (node-antinode pattern inside the chamber) has to be studied in more detail, and in the following analysis we just have to consider its presence while interpreting the results.

Our microphone<sup>3)</sup> has a frequency response characteristic flat within  $\pm 1$  dB in a frequency range 6 Hz – 10 kHz, and within  $\pm 2$  dB in a frequency range of 4 Hz – 40 kHz.

A complete block scheme of the experiment is presented in fig. 2.

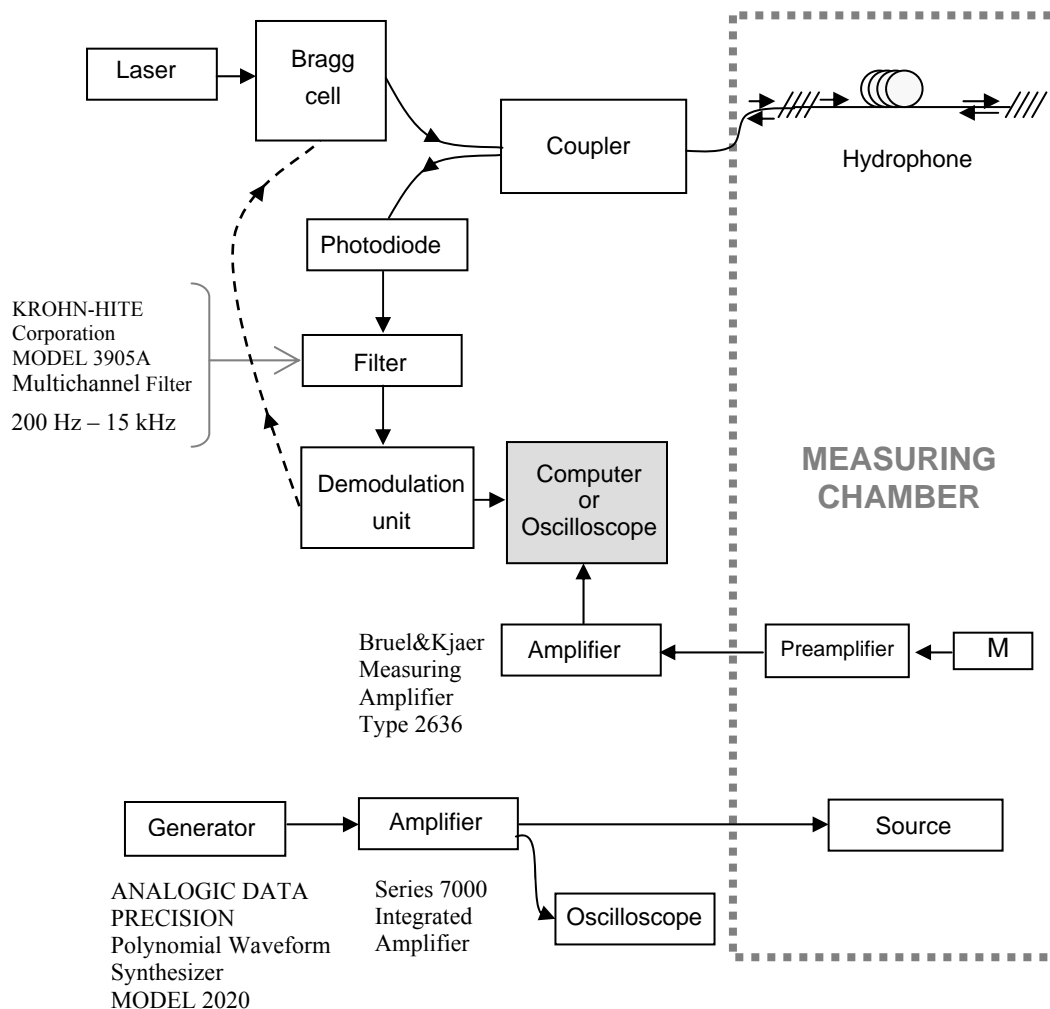


**FIG. 2:** Block scheme of the experiment.

The response of the hydrophone and of the microphone was measured at different

signal frequencies emitted by the source. Frequency range was from 1 to 10 kHz with a 0.5 kHz step. For small enough signals, using a 23.9 kHz carrier, the demodulation unit has a linear response up to 10 kHz, so it was an upper limit for our analysis. The data was recorded in form of spectral dependencies (response depending on frequency). For each source signal frequency and each detector arrangement (a)-(d) a series of 30 or 50 measurements was performed and an averaged data set was recorded. In total 6 data sets were recorded (H1, M1, H2, M2, H3, M3, see fig.1).

### 3 HOW A FIBER OPTIC HYDROPHONE WORKS

#### 3.1 The interference

Hydrophone measuring system consists of a laser source, a Bragg cell, a coupler, a photodiode and an optic fiber line with a hydrophone and two Fiber Bragg grating mirrors in it, one located before the hydrophone and the other one after (see fig. 2). Reflection ratios of the mirrors are 1.5% and 20% respectively. Acoustic pressure is determined by observing interference between two laser pulses reflected from the mirrors. The two pulses come with a time interval  $\tau$ , which is equal to the time of signal propagation to the end of the hydrophone line and back. The interference is observed between the first pulse A reflected from the mirror 2 and the second pulse B reflected from the mirror 1 (fig. 3). Other reflected signals are not taken into account.

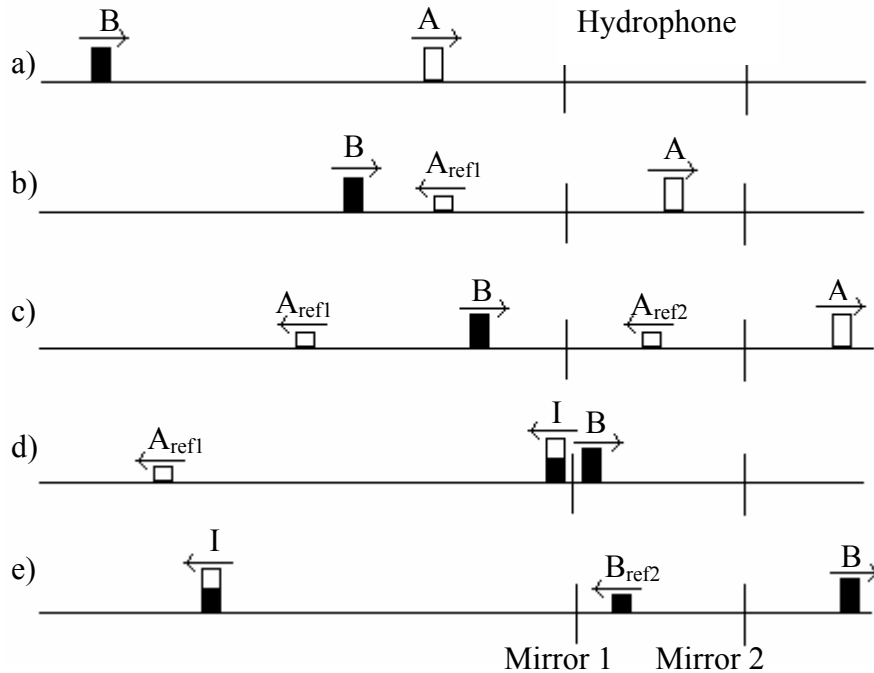


**FIG. 3:** Interference of the two laser pulses in a hydrophone line. A and B are the initial pulses,  $A_{ref1}$ ,  $A_{ref2}$ ,  $B_{ref1}$  are the pulses reflected from mirrors 1 and 2 respectively, I is the result of interference between pulses  $A_{ref2}$  and  $B_{ref1}$  (not shown at the figure).

### 3.2 The Bragg cell

A beam from a continuous wave laser source with a wavelength of 1319 nm enters the Bragg cell<sup>4)</sup>, which outputs a sequence of two laser pulses with slightly different wavelengths (frequencies).

In our case, the laser beam is modulated by a sequence of ultrasound pulses, as shown in fig. 4. Thus, the Bragg cell output is two laser pulses with frequencies different by  $\Delta F$  with a preset time interval between them.

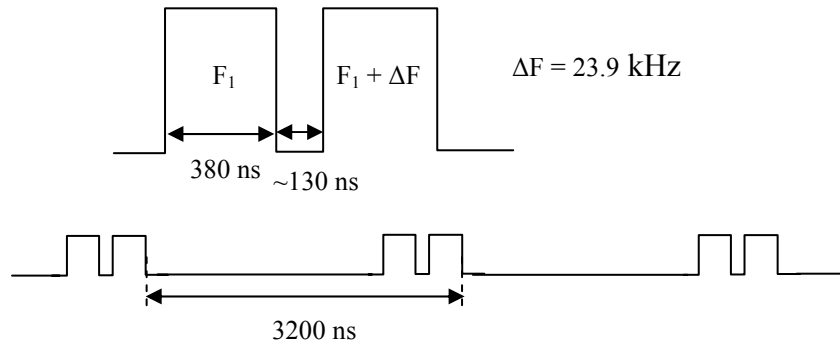


FIG. 4: Sketch of the modulating pulses inside the Bragg cell.

### 3.3 Retrieving the pressure

When the hydrophone is exposed to acoustic pressure, the optic fiber changes its length  $L$  and refractive index  $n$ , resulting in an optical path length change for the laser pulse passing through the hydrophone. It means that the pulse gains an extra phase shift dependent on pressure at the moment of measurement. This phase shift is given by<sup>5)</sup>

$$\frac{d\varphi}{\varphi} = \xi \varepsilon, \quad (1)$$

or

$$d\varphi = \frac{2\pi n L \xi \varepsilon}{\lambda}, \quad (2)$$

where  $\varepsilon = dL/L$ ,  $L$  is the physical path length and

$$\xi = 1 - \frac{1}{2} n^2 P_{12} \approx 0.71 \quad (3)$$

is the decrease of the phase shift due to the refractive index change ( $P_{12}$  is the strain optic coefficient, for silica  $P_{12} = 0.27$ ).

The result of interference of two laser pulses can be written as follows<sup>5)</sup>:

$$I = I_0 [1 + V \cos(2\pi f_c t + \Phi(t))] \quad (4)$$

Here  $f_c = \Delta F$  is the carrier frequency. It is determined by the frequency difference between two laser pulses coming out of the Bragg cell, so its value is preset and introduced as a parameter into the read-out system program.  $\Phi(t)$  is a phase shift induced by the acoustic pressure affecting the hydrophone and  $V$  stands for visibility of the interference.  $\Phi(t)$  can be retrieved as a result of demodulation performed by the data processing system.

The results of measuring hydrophone response to acoustic signal were represented in volts. A calibration procedure for the read-out system was conducted to establish an interconnection between initial phase shift in radians and output in volts.

## 4 CALIBRATION AND RESULTS

### 4.1 Calibration of the electronic read-out system

To calibrate the read-out system for different frequencies, the synthetic signal  $I$  was put into the AD converter:

$$I = 0.8 \sin(2\pi \cdot 23,9 \text{ KhZ} \cdot t + 0.1 \sin(1 \text{ kHz} \cdot t)). \quad (5)$$

Here 23.9 kHz is carrier frequency, the second term in brackets is a simulation of a periodical pressure influence with 1 kHz frequency and 0.1 rad (= 100 mrad) amplitude. A corresponding hydrophone response in decibel volts (dBV) was determined. The same procedure was repeated with 10 mrad amplitude and for frequencies up to 10 kHz with a 0.5 kHz step. From this data a demodulation stage response of the read-out system in V/rad units was calculated for each frequency.

### 4.2 Calibration of the hydrophone and the responsivity calculation

Having calibrated the electronic read-out system, we performed the calibration of the hydrophone using the absolute data we had for the microphone. We assumed that the signal amplitude for a given signal frequency is the same in the same spatial point, so the hydrophone in each of 3 positions inside the chamber was calibrated with the microphone data set corresponding to the microphone location in the same position, i.e. H1 with M2 and H2 with M1.

In the calculation we considered amplification settings for the microphone (+33 dB), microphone sensitivity  $S_0 = -38 \text{ dB re } 1\text{V/Pa}$  and for each signal frequency emitted by the source we determined signal amplitude in  $\mu\text{Pa}$  from the microphone data. Using the above-described read-out system response in V/rad for each frequency, we calculated the hydrophone response in rad. As a result, we determined the hydrophone responsivity in [dB re rad/ $\mu\text{Pa}$ ] units for signal frequencies from 1 to 10 kHz with a 0.5 kHz step for 3 different positions of the hydrophone inside the chamber.

In fig. 5 frequency responsivity averaged over 3 hydrophone positions is presented.

For each frequency  $f_i = 1, 1.5, 2 \dots, 10$  kHz we calculated the mean responsivity  $\mu_i$  (plotted in fig. 5) and its standard deviation  $\sigma_i$ . Then we fitted these standard deviations  $\{\sigma_i\}$  with the normal distribution and determined the mean  $\mu$  and the standard deviation  $\sigma$ . The final value of the error was evaluated as  $(\mu + \sigma)$  and was assigned to all frequency points.

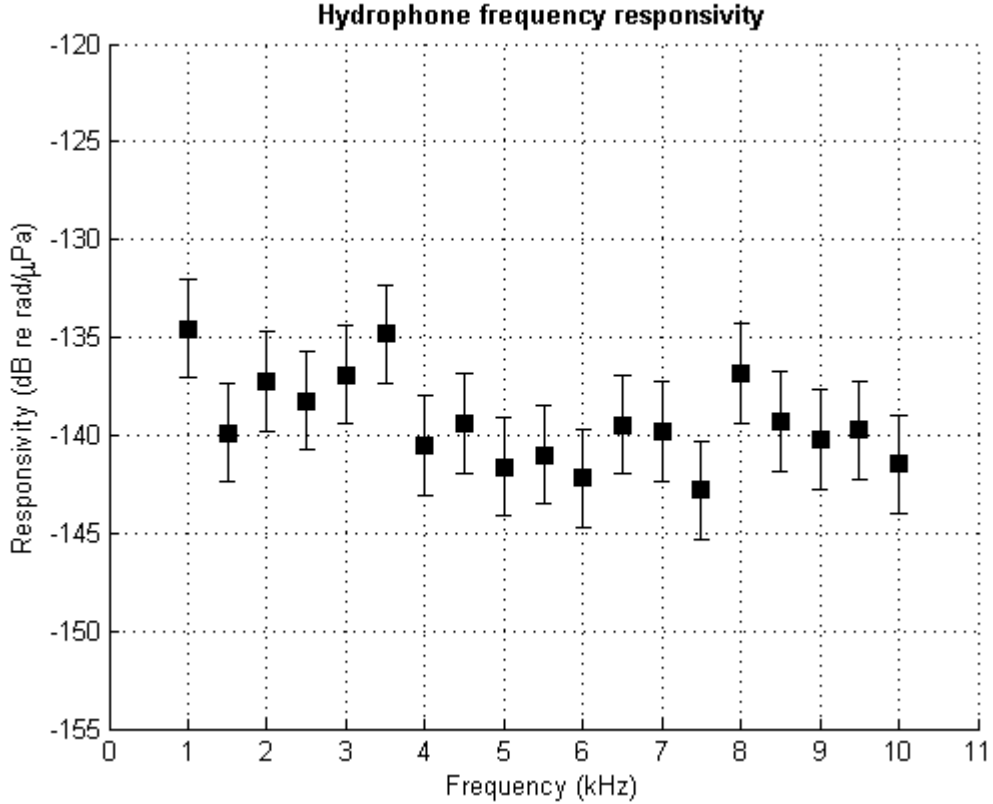


**FIG. 5:** Hydrophone frequency responsivity averaged over 3 positions of the hydrophone inside the chamber.

For comparison, the frequency responsivity was estimated also with a different procedure. The plot in fig. 6 is the result of averaged near field measurements at different positions (distance emitter-receiver) with pink noise on the microphone and the hydrophone separately. Let  $X$  the loudspeaker input and  $Y$  the receiver output (microphone or hydrophone). Every measurement is obtained by averaged cross spectrum to averaged autospectrum ratio:  $\langle YX^* \rangle / \langle XX^* \rangle$ . At very low frequencies the coherence function has low values, so the plot at these frequencies has to be ignored. The uncertainties in this case were not specified, but we assume them not to exceed the errors of the previous measurement.

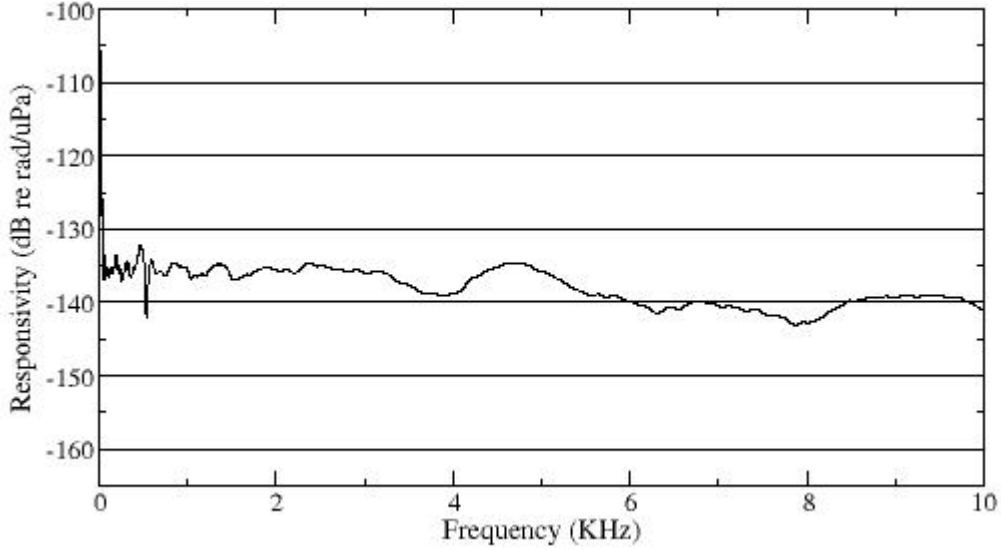


**FIG. 6:** Hydrophone frequency responsivity estimated with a different procedure.

Comparing fig. 5 and 6, we can conclude that there is a good agreement between hydrophone responsivities obtained with different techniques. The frequency responsivity characteristic can be considered flat within  $\pm 6$  dB in a frequency range 1–10 kHz. The responsivity value averaged over this frequency range is  $(139.3 \pm 2.3)$  dB re rad/ $\mu$ Pa.

In our previous report<sup>1)</sup> we calculated the expected responsivity of our prototype using the elastic theory and we found that its value was

$$\Delta\varphi/(\varphi P) = -309 \text{ dB re } 1/\mu\text{Pa}. \quad (6)$$

To estimate the agreement between the calculated value (6) and the experimentally achieved responsivity  $\Delta\varphi/P = -139$  dB re rad/ $\mu$ Pa, we transform them into the same units. Considering that

$$\varphi = \frac{2\pi n L}{\lambda}, \quad (7)$$

where  $L = 32$  m is the total winded length of the optic fiber,  $n = 1.5$  is the refraction index and  $\lambda = 1319$  nm is the wavelength of the light emitted by the laser, we obtain that the theoretically calculated responsivity (6) is equivalent to  $\Delta\varphi/P = -142$  dB re rad/ $\mu$ Pa in agreement with the average experimental value within 3 dB.

## 5 MINIMUM DETECTABLE SIGNAL ESTIMATION

We have measured the response of the hydrophone to a 5 kHz signal emitted by the sound source at different amplitudes of the emitted signal varied in the range from 0.1 V to 0.0025 V. The hydrophone was located in position H3. In fig. 7 hydrophone response to the lowest achieved source signal amplitude is presented.

The minimum detectable signal value was obtained by fitting the noise level around

5 kHz with normal distribution and assuming that the signal is detectable if its amplitude exceeds  $(\mu + 3\sigma)$  of the noise level. The results of the normal fit are shown in fig. 8. Here the mean noise value was obtained over the frequency range 4900-5100 Hz with the peak region excluded. The minimum detectable signal from the above-given definition is  $\mu + 3\sigma = -81.7$  dB re V. It is denoted by a red cross in fig. 7. Since we know the responsivity of our hydrophone, we can determine that it stands for the pressure amplitude of 0.6 mPa.

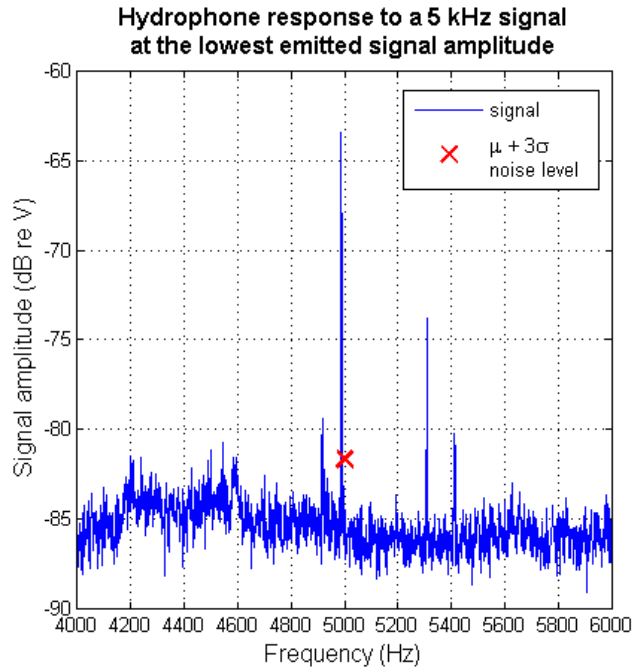


**FIG. 7:** Hydrophone response to a 5 kHz signal at the lowest emitted signal amplitude. The red cross denotes the minimum detectable signal level (determined in the text).

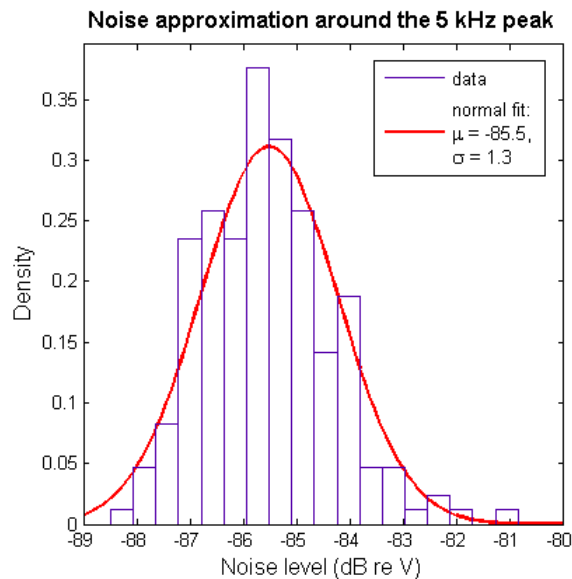


**FIG. 8:** Fitting of the noise around the 5 kHz peak with normal distribution.

## **8 REFERENCES**

- (1) Technical report INFN-TC-06-14 (November 2006).
- (2) Technical report INFN-TC-06-17 (December 2006).
- (3) Brüel&Kjaer Condenser Microphone Type 4133 Calibration Chart.
- (4) Encyclopedia of Laser Physics and Technology,  
<http://www.rp-photonics.com/encyclopedia.html>.
- (5) C. K. Kirkendall, A.Dandridge, J. Phys. D.: Appl. Phys. **37**, pp. 197-216, (2004).